Mitigating Heat Dissipation in Raman Lasers Using Coherent Anti-Stokes Raman Scattering

Nathalie Vermeulen,[1] Christof Debaes,[1] Peter Muys,[2] and Hugo Thienpont[1]
[1]*Department of Applied Physics and Photonics, Vrije Universiteit Brussel, B-1050 Brussels, Belgium*
[2]*Lambda Research Optics Europe, B-9810 Eke, Belgium*
(Received 15 November 2006; published 28 August 2007)

We present a novel technique that intrinsically mitigates the quantum-defect heating in Raman lasers. The basic principle of this so-called ''coherent anti-Stokes Raman scattering (CARS)-based heat mitigation'' is to suppress the phonon creation in the Raman medium by increasing the number of out-coupled anti-Stokes photons with respect to the number of out-coupled Stokes photons. We demonstrate with the aid of numerical simulations that for a hydrogen and a silicon Raman laser, CARS-based heat mitigation efficiencies of at least 30% and 35%, respectively, can be obtained.

DOI: 10.1103/PhysRevLett.99.093903 PACS numbers: 42.55.Ye, 42.65.Dr

An important issue when operating optically pumped lasers is the heat dissipation inside the active medium due to the quantum defect between the pump and the lasing wavelength. The resulting increase in temperature can have detrimental consequences for the laser performance, such as a decrease of the lasing efficiency and a deterioration of the lasing medium and/or the beam quality. Most of the conventional heat disposal techniques based on water or air cooling are not ideal from the point of view of downscaling the laser volume, of preventing thermally induced refractive index changes, and in the case of a solid medium, of mitigating thermally induced stresses. Improving the thermal management in a laser medium is therefore key to a higher reliability and lifetime of the laser and/or a route to further laser miniaturization. To that aim, intrinsic heat mitigation mechanisms should be used that, instead of disposing of the heat when it has reached the outer surface of the active medium, minimize the heat generation already inside the medium.

Over the past decade, much progress has been made in the field of so-called ''anti-Stokes fluorescence cooling'' [1–3]. Hereby, solid-state materials are cooled down by the conversion of incoming pump photons into higher energy anti-Stokes fluorescence photons. This process results in the annihilation of phonons inside the material and as such decreases the material's temperature. Bowman has shown that anti-Stokes fluorescence cooling can also be used indirectly for suppressing the heat generation in an active lasing medium [4]. He conceptualized the so-called ''radiation-balanced laser'', containing an active medium in which sufficient anti-Stokes fluorescence cooling can be obtained to cancel the quantum-defect heating that accompanies the laser emission process. A successful application of anti-Stokes fluorescence cooling requires, among others, that the solid-state material allows pumping at a frequency smaller than its average fluorescence frequency and can as such only be achieved in a limited number of active media such as Yb^{3+}-doped [1], Tm^{3+}-doped [2], and Er^{3+}-doped [3] crystals and glasses. Raman media inherently do not feature a fluorescence band, so this large family of lasing materials certainly can not take advantage neither of anti-Stokes fluorescence cooling nor of radiation-balanced lasing. Therefore, to intrinsically mitigate the heat dissipation in Raman lasers, a new approach is needed that is based on a different mechanism than anti-Stokes fluorescence cooling.

In this Letter, we present such a novel technique which is based on coherent anti-Stokes Raman scattering (CARS). In the Raman medium of a Raman laser, three different scattering processes can take place, being stimulated Stokes Raman scattering (SSRS), stimulated anti-Stokes Raman scattering (SARS), and CARS. We consider here the commonly used working point of maximal Raman gain, which implies that the Raman medium features no population inversion between the material oscillation energy level $|f\rangle$ and the ground energy level $|i\rangle$ shown in Fig. 1, and that the mentioned scattering processes are exactly at Raman resonance [5,6]. The first process, SSRS, is the actual lasing mechanism of Raman lasers and is schematically represented in Fig. 1(a). During this Raman interaction, an incoming pump photon scatters onto an internal material oscillation such as, e.g., a molecular vibration, and this scattering event results both in the

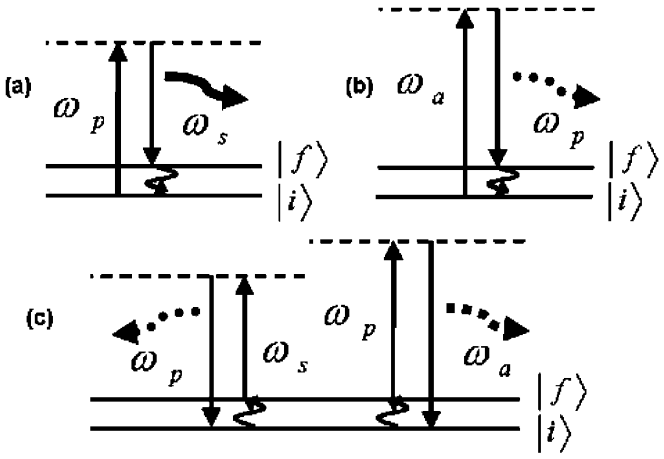

FIG. 1. Schematic representation of the photon and phonon balances of (a) SSRS, (b) SARS, (c) CARS converting a Stokes photon into an anti-Stokes photon.

creation of a lower energy Stokes photon and in the generation of a phonon or heat, i.e., quantum-defect heating. Then, the SARS process converts an anti-Stokes photon into a pump photon and a phonon, as shown in Fig. 1(b). As such, it generates quantum-defect heating in the same way as SSRS. Finally, CARS at Raman resonance is, as we will show later on, a four-wave mixing process that—in case of perfect phase matching—converts a pump photon and a Stokes photon into a pump photon and an anti-Stokes photon, while annihilating two phonons [5,7]. This process, which reduces the quantum-defect heating in the Raman medium, is visualized in Fig. 1(c). In case of a phase mismatch, the induced phase variation along the fields' propagation path will cause the process shown in Fig. 1(c) to alternate with the reverse mechanism [5]. This point of view is very different from the most common interpretation of CARS, where it is seen as a mechanism that converts two pump photons into a Stokes and an anti-Stokes photon without exchanging energy with the Raman medium.

Let us now combine the photon and phonon balances of the above mentioned Raman processes and assume that the laser has reached its steady-state regime. We then find that the ratio of the number of anti-Stokes photons to the number of Stokes photons, coupled out of the Raman laser, indicates how much the quantum-defect heating in the laser is reduced compared to the quantum-defect heating generated in a SSRS-based Raman laser to produce the same amount of Stokes lasing photons. In other words, this photon number ratio corresponds to the ratio with which the average quantum-defect heating per out-coupled Stokes photon is reduced with respect to the quantum-defect heating per out-coupled Stokes photon in a SSRS-based Raman laser. To effectively mitigate the quantum-defect heating in a Raman laser, we should therefore increase the ratio of the number of out-coupled anti-Stokes photons to the number of out-coupled Stokes photons. Because of the importance of the anti-Stokes-creation by CARS in this approach, we termed it "CARS-based heat mitigation."

To investigate the efficiency of CARS-based heat mitigation, we make use of the Stokes–anti-Stokes iterative resonator method that we developed, starting from the well-known expressions for Raman-resonant SSRS, SARS, and CARS in a noninverted medium [6], for modeling continuous-wave Raman lasers [8]. This modeling method reevaluates for every half round-trip time the longitudinal pump, Stokes, and anti-Stokes electric field distributions inside the cavity until the steady-state regime is reached. Let us consider a Raman laser cavity with length L and with front and back mirror reflectivities $R_{\{p,s,a\},\mathrm{front}}$ and $R_{\{p,s,a\},\mathrm{back}}$ at the pump, Stokes, and anti-Stokes wavelengths λ_p, λ_s, λ_a, respectively. Applying for a certain half round-trip (α) the Stokes–anti-Stokes iterative resonator method [8] to the amplitudes of the intracavity pump fields $E^+_{p,(\alpha)}(z)$ and $E^-_{p,(\alpha)}(z)$, Stokes fields $E^+_{s,(\alpha)}(z)$ and $E^-_{s,(\alpha)}(z)$, and anti-Stokes fields $E^+_{a,(\alpha)}(z)$ and $E^-_{a,(\alpha)}(z)$, propagating in the forward and the backward direction, respectively, yields the following equations:

$$\frac{\partial E^{\pm}_{p,(\alpha)}}{\partial z} = \mp\left[\frac{\lambda_s}{\lambda_p}(G^{\pm}_s|E^+_{s,(\alpha)}|^2 + G^{\mp}_s|E^-_{s,(\alpha)}|^2)\right]E^{\pm}_{p,(\alpha)} \pm [(G^{\pm}_p|E^+_{a,(\alpha)}|^2 + G^{\mp}_p|E^-_{a,(\alpha)}|^2)]E^{\pm}_{p,(\alpha)} - \gamma^{\pm}_p E^{\pm}_{p,(\alpha)}, \tag{1}$$

$$\frac{\partial E^{\pm}_{s,(\alpha)}}{\partial z} = \pm[G^{\pm}_s|E^+_{p,(\alpha)}|^2 + G^{\mp}_s|E^-_{p,(\alpha)}|^2]E^{\pm}_{s,(\alpha)} \pm \left[\frac{\lambda_a}{\lambda_s}C_{sa}(E^{\pm}_{p,(\alpha)})^2(E^{\pm}_{a,(\alpha)})^* e^{\pm i\Delta k(z+\Lambda)}\right] - \gamma^{\pm}_s E^{\pm}_{s,(\alpha)}, \tag{2}$$

$$\frac{\partial E^{\pm}_{a,(\alpha)}}{\partial z} = \mp\left[\frac{\lambda_p}{\lambda_a}(G^{\pm}_p|E^+_{p,(\alpha)}|^2 + G^{\mp}_p|E^-_{p,(\alpha)}|^2)\right]E^{\pm}_{a,(\alpha)} \mp [C_{sa}(E^{\pm}_{p,(\alpha)})^2(E^{\pm}_{s,(\alpha)})^* e^{\pm i\Delta k(z+\Lambda)}] - \gamma^{\pm}_a E^{\pm}_{a,(\alpha)}. \tag{3}$$

Here, the SSRS-related Stokes gain coefficients for forward and backward SSRS , G^+_s, G^-_s, the SARS-related pump gain coefficients for forward and backward SARS G^+_p, G^-_p, and the CARS-related coupling coefficient C_{sa} obey, for a pump linewidth $\Delta\nu_p$ within the limits set by dispersion [9–11], the equations

$$G^+_s = \frac{1}{4}g\left(\frac{\varepsilon_0}{\mu_0}\right)^{1/2}; \qquad G^+_p = \frac{\lambda_s}{\lambda_p}G^+_s; \qquad C_{sa} = \frac{\lambda_s}{\lambda_a}G^+_s; \qquad G^-_{\{s,p\}} = \frac{G^+_{\{s,p\}}}{1+\Delta\nu_p/\Delta\nu_R}. \tag{4}$$

Here, g indicates the Raman gain coefficient and $\Delta\nu_R$ represents the spontaneous Raman linewidth. $\gamma^{\pm}_p$, $\gamma^{\pm}_s$, and $\gamma^{\pm}_a$ are the medium-dependent optical losses of the pump, Stokes, and anti-Stokes fields, whereas the total power losses integrated over the cavity length at half round-trip (α) will be represented further on in this Letter by the electric field amplitudes $E^{\mathrm{loss}}_{p,(\alpha)}$, $E^{\mathrm{loss}}_{s,(\alpha)}$, and $E^{\mathrm{loss}}_{a,(\alpha)}$, respectively. We remark that these electric fields also contribute to the out-coupled photon numbers discussed earlier. Furthermore, $\overline{\Delta k} = 2\bar{k}_p - \bar{k}_s - \bar{k}_a$ is the wave-vector-dependent phase mismatch of the CARS-process and Λ equals the total distance that the fields have traversed inside the cavity over all the previous half round-trips. Finally, the boundary conditions at the front and back cavity mirrors that link the successive half round-trips, and the expressions for the field amplitudes $E^{\{\mathrm{front,back}\}}_{\{p,s,a\},(\alpha)}$ emitted through the cavity mirrors can be found in [8] and will not be repeated here.

When we multiply Eqs. (2) and (3) with $(E^{\pm}_{s,(\alpha)})^*$ and $\frac{\lambda_a}{\lambda_s}(E^{\pm}_{a,(\alpha)})^*$, respectively, and sum these equations, we find

that the sum of the number of Stokes and anti-Stokes photons does not depend on the CARS process. This means that the interpretation as if CARS at Raman resonance would be a mechanism that converts two pump photons into a Stokes and an anti-Stokes photon is incorrect. Furthermore, we can deduce from Eqs. (2) and (3) that in case $\Delta k = 0$, the interplay of the SSRS, SARS, and CARS terms causes the Stokes and anti-Stokes fields to dephase, regardless their initial phase conditions. Moreover, we find that the nature of this dephasing is such that the CARS term in Eq. (3) increases the number of anti-Stokes photons at the expense of the Stokes fields which experience loss through the CARS term in Eq. (2). This process is accompanied by phonon annihilation and is also responsible for the so-called gain suppression of the Stokes fields at phase matching, a phenomenon that cannot be explained using the commonly used interpretation of CARS [5,7]. In case Δk is different from zero, the phase of the CARS terms in Eqs. (2) and (3) will vary along the field's propagation path, which causes the process described above to alternate with the reverse process, where Stokes photons are created at the expense of anti-Stokes photons and where phonons are generated [5]. We thus find that, when working at exact Raman resonance in a noninverted medium, the CARS process does exchange energy with the Raman medium.

We remark that away from Raman resonance, the commonly used CARS-scheme will become valid [5], but since the latter corresponds to Stokes generation without quantum-defect heating, the general concept of CARS-based heat mitigation will still apply. We also note that our novel CARS interpretation is not valid for the Raman experiments conducted in media with electromagnetically induced transparency [12,13], since the working conditions in such media are far different from those in ''plain'' media that are not coherently prepared, as we consider in this Letter.

Using the modeling formalism described above, we can determine the total quantum-defect heating H at the half round-trip (α) by integrating the powers dP, that are dissipated along the cavity, over the cavity length L. Taking into account that $\frac{dP}{dz} = \mathrm{Re}(E^* \frac{dE}{dz}) \frac{A}{\mu_0 c}$, where A represents the modal effective area, we obtain that H for a Raman laser in which SSRS, SARS, and CARS simultaneously occur, equals

$$H = \frac{A}{\mu_o c}\Bigg\{\int_{z=0}^{z=L} \sum_{\tau=+,-} [[1]_{(1),\tau}|E^{\tau}_{p,(\alpha)}|^2 - [1]_{(2),\tau}|E^{\tau}_{s,(\alpha)}|^2]dz + \int_{z=0}^{z=L} \sum_{\tau=+,-} [[1]_{(3),\tau}|E^{\tau}_{a,(\alpha)}|^2 - [2]_{(1),\tau}|E^{\tau}_{p,(\alpha)}|^2]dz + \int_{z=0}^{z=L} \sum_{\tau=+,-} [\mathrm{Re}([2]_{(3),\tau}(E^{\tau}_{a,(\alpha)})^*) - \mathrm{Re}([2]_{(2),\tau}(E^{\tau}_{s,(\alpha)})^*)]dz\Bigg\}. \quad (5)$$

Here, $[x]_{(y),\tau}$ indicates the xth term in square brackets from equation (y) on the previous page, that corresponds to forward propagation if $\tau = +$ and to backward propagation if $\tau = -$. A good figure of merit for CARS-based heat mitigation is the ratio with which the average quantum-defect heating per out-coupled Stokes photon is reduced compared to the corresponding quantum-defect heating in a SSRS-based Raman laser. Assuming steady-state laser operation, we find that this figure of merit or ''CARS-based heat mitigation efficiency'' η_{HM} can be expressed as

$$\eta_{\mathrm{HM}} = \frac{|E^{\mathrm{front}}_{a,(\alpha)}|^2 + |E^{\mathrm{back}}_{a,(\alpha)}|^2 + |E^{\mathrm{loss}}_{a,(\alpha)}|^2}{|E^{\mathrm{front}}_{s,(\alpha)}|^2 + |E^{\mathrm{back}}_{s,(\alpha)}|^2 + |E^{\mathrm{loss}}_{s,(\alpha)}|^2} \frac{\omega_s}{\omega_a} \times 100\%. \quad (6)$$

To obtain a large value for η_{HM} without compromising the Stokes lasing power, many anti-Stokes photons need to be generated. First, one can strengthen the anti-Stokes generation through CARS by realizing phase matching or $\Delta k = 0$. Second, from Eqs. (3) and (4) we know that for pump linewidth values within the limits set by dispersion—these limits determine the pump linewidth values for which the pump field still coherently propagates with the Stokes and anti-Stokes fields but only in the copropagating scattering direction—the gain of backward Raman scattering will decrease with increasing pump linewidth whereas the gain of forward Raman scattering will remain unchanged. Thus, when increasing the pump linewidth, fewer anti-Stokes photons are ''absorbed'' by backward SARS, whereas the efficiency of the forward SSRS lasing process does not decrease.

To demonstrate the feasibility of our CARS-based heat mitigation technique, we will now calculate η_{HM} for two different types of Raman lasers. Let us first assume a H_2-based Raman laser consisting of a hollow-core photonic crystal fiber (HC PCF) that is filled with H_2 and spliced at both sides to a piece of standard fiber that contains a Bragg grating [11,14,15]. Let us further assume that we pump it with a 30 W continuous-wave frequency doubled Nd:YAG laser ($\lambda_p = 532$ nm) with a relatively large pump linewidth $\Delta\nu_p = 2$ GHz [16]. The remaining parameter values used for our numerical simulations are: $\lambda_s = 683$ nm, $\lambda_a = 436$ nm (both wavelength shifts with respect to λ_p correspond to the $Q(1)$ vibrational transition in H_2), $g = 2.95 \times 10^{-9}$ cm/W [17], $\Delta\nu_R = 650$ MHz [17], $L = 20$ cm, $A = 80\ \mu\mathrm{m}^2$, $\gamma_p^{\pm} = \gamma_s^{\pm} = \gamma_a^{\pm} = \pm 0.01$ dB/m [18], $R_{\{p,a\},\mathrm{front}} = R_{\{p,a\},\mathrm{back}} = 0$, $R_{s,\mathrm{front}} = R_{s,\mathrm{back}} = 0.6$ and splice losses of 0.6 dB [14]. We may also assume that phase matching ($\Delta k = 0$) can be obtained in the HC PCF [19]. When using these parameter values for our numerical simulations, we obtain that the steady-state values for the pump, Stokes, and anti-Stokes powers emitted through the cavity mirrors equal 22.01, 0.32, and 0.21 W, respectively. Using Eqs. (5) and (6), we find that H per half round-trip in the steady-state regime equals 0.101 W which is 12% of the converted pump power, and

that $\eta_{\mathrm{HM}} = 30\%$. Taking into account that the total out-coupled Stokes power (including losses) in the steady-state regime equals 0.507 W and that for a H_2 Raman laser based on SSRS each out-coupled Stokes photon would correspond to 0.516 eV of dissipated energy, we indeed see that the average quantum-defect heating per out-coupled Stokes photon is reduced with $\eta_{\mathrm{HM}} = 30\%$. When we consider the laser as a dual-wavelength source, we obtain an external lasing efficiency of $(0.32 + 0.21)$ W/30 W = 1.8%.

In a second example, we calculate η_{HM} for a Si-based Raman laser. Here, we consider the particular case of a silicon-on-insulator waveguide Raman laser since also this guiding structure is suitable for obtaining the phase matching condition $\Delta k = 0$ [20]. Let us assume that the pump source is a 5 W continuous-wave fiber laser featuring $\lambda_p = 2.7\ \mu$m and $\Delta\nu_p = 300$ GHz [21]. Pumping Si-based Raman lasers at a mid-infrared wavelength has several advantages, such as the absence of two-photon absorption and free carrier absorption [22]. The remaining parameter values are $\lambda_s = 3.14\ \mu$m, $\lambda_a = 2.37\ \mu$m, $g = 1.6 \times 10^{-8}$ cm/W [23], $\Delta\nu_R = 105$ GHz [23], $L = 2.5$ cm, $A = 3\ \mu\mathrm{m}^2$, $\gamma_p^{\pm} = \gamma_s^{\pm} = \gamma_a^{\pm} = \pm 1$ dB/cm, $R_{p,\mathrm{front}} = R_{p,\mathrm{back}} = 0.05$, $R_{s,\mathrm{front}} = R_{s,\mathrm{back}} = 0.45$, $R_{a,\mathrm{front}} = R_{a,\mathrm{back}} = 0$, and $\Delta k = 0$. Implementing these parameter values in our numerical simulations yields steady-state values for the pump, Stokes, and anti-Stokes powers emitted through the cavity mirrors of 1.41, 0.69, and 0.43 W, respectively. Using Eqs. (5) and (6), we now obtain that H per half round-trip in the steady-state regime equals 0.135 W which is 7% of the converted pump power, and that $\eta_{\mathrm{HM}} = 35\%$. Here, the external lasing efficiency comprising both the Stokes and anti-Stokes emitted powers is, despite the gain suppression at phase matching, as high as 22%.

We would like to remark that even for considerable phase mismatches such as $2\pi/(2 \times 20\ \mathrm{cm}) = 0.16\ \mathrm{cm}^{-1}$ and $2\pi/(2 \times 2.5\ \mathrm{cm}) = 1.26\ \mathrm{cm}^{-1}$ for the H_2- and Si-based Raman lasers, respectively, we obtain that η_{HM} is still as high as 9% and 12%.

In summary, we have introduced a novel CARS-based heat mitigation mechanism for Raman lasers that, when applied to a H_2- and a Si-based Raman laser, can reduce the average quantum-defect heating per out-coupled Stokes photon by at least 30% and 35%, respectively, with respect to the corresponding heating in a Raman laser based on SSRS only.

This work was supported in part by the Fund for Scientific Research-Flanders (FWO-Vlaanderen), by IAP BELSPO, by the European Network of Excellence on Micro-Optics NEMO, by GOA, and by OZR of Vrije Universiteit Brussel. Nathalie Vermeulen and Christof Debaes are indebted to FWO-Vlaanderen for an Aspirant grant and a Postdoctoraal Onderzoeker grant, respectively.

[1] R. I. Epstein *et al.*, Nature (London) **377**, 500 (1995).
[2] C. W. Hoyt *et al.*, Phys. Rev. Lett. **85**, 3600 (2000).
[3] J. Fernandez, A. J. Garcia-Adeva, and R. Balda, Phys. Rev. Lett. **97**, 033001 (2006).
[4] S. R. Bowman, IEEE J. Quantum Electron. **35**, 115 (1999).
[5] B. Bobbs and C. Warner, J. Opt. Soc. Am. B **7**, 234 (1990).
[6] N. S. Makarov and V. G. Bespalov, J. Opt. A Pure Appl. Opt. **5**, S250 (2003).
[7] R. Chiao and B. P. Stoicheff, Phys. Rev. Lett. **12**, 290 (1964).
[8] N. Vermeulen *et al.*, IEEE J. Quantum Electron. **42**, 1144 (2006).
[9] W. R. Trutna, Y. K. Park, and R. L. Byer, IEEE J. Quantum Electron. **15**, 648 (1979).
[10] K. Sentrayan, A. Michael, and V. Kushawaha, Appl. Opt. **32**, 930 (1993).
[11] F. Benabid, J. C. Knight, G. Antonopoulos, and P. St. J. Russell, Science **298**, 399 (2002).
[12] A. J. Merriam *et al.*, IEEE J. Sel. Top. Quantum Electron. **5**, 1502 (1999).
[13] C. H. van der Wal *et al.*, Science **301**, 196 (2003).
[14] F. Benabid *et al.*, Nature (London) **434**, 488 (2005).
[15] F. Couny, F. Benabid, and O. Carraz, J. Opt. A Pure Appl. Opt. **9**, 156 (2007).
[16] P. K. Mukhopadhyay *et al.*, Opt. Commun. **259**, 805 (2006).
[17] W. K. Bischel and M. J. Dyer, J. Opt. Soc. Am. B **3**, 677 (1986).
[18] P. J. Roberts *et al.*, Opt. Express **13**, 236 (2005).
[19] S. O. Konorov, A. B. Fedotov, A. M. Zheltikov, and R. B. Miles, J. Opt. Soc. Am. B **22**, 2049 (2005).
[20] D. Dimitropoulos, V. Raghunathan, R. Claps, and B. Jalali, Opt. Express **12**, 149 (2004).
[21] X. Zhu and R. Jain, Appl. Opt. **45**, 7118 (2006).
[22] V. Raghunathan, R. Shori, O. M. Stafsudd, and B. Jalali, Phys. Status Solidi A **203**, R38 (2006).
[23] B. Jalali, R. Claps, D. Dimitropoulos, and V. Raghunathan, *Light Generation, Amplification, and Wavelength Conversion via Stimulated Raman Scattering in Silicon Microstructures*, edited by L. Pavesi and D. J. Lockwood, Silicon Photonics (Springer-Verlag, Germany, 2004).